Toxicology in Vitro 24 (2010) 728–736

Contents lists available at ScienceDirect

Toxicology in Vitro

journal homepage: www.elsevier.com/locate/toxinvit

Calcium signals and caspase-12 participated in paraoxon-induced apoptosis in EL4 cells

Lan Li, Zhiheng Cao, Pengfei Jia, Ziren Wang *

School of Life Sciences, Lanzhou University, Lanzhou 730000, PR China

ARTICLE INFO

Article history:
Received 19 July 2009
Accepted 11 January 2010
Available online 15 January 2010

Keywords:
Paraoxon
EL4 cells
Apoptosis
Calcium signals
Endoplasmic reticulum
Caspase-12

ABSTRACT

In order to investigate whether calcium signals participate in paraoxon (POX)-induced apoptosis in EL4 cells, real-time laser scanning confocal microscopy (LSCM) was used to detect Ca^{2+} changes during the POX application. Apoptotic rates of EL4 cells and caspase-12 expression were also evaluated. POX (1–10 nM) increased intracellular calcium concentration ($[Ca^{2+}]i$) in EL4 cells in a dose-dependent manner at early stage (0–2 h) of POX application, and apoptotic rates of EL4 cells after treatment with POX for 16 h were also increased in a dose-dependent manner. Pre-treatment with EGTA, heparin or procaine attenuated POX-induced $[Ca^{2+}]i$ elevation and apoptosis. Additionally, POX up-regulated caspase-12 expression in a dose-dependent manner, and pre-treatment with EGTA, heparin or procaine significantly inhibited POX-induced increase of caspase-12 expression. Our results suggested that POX induced $[Ca^{2+}]i$ elevation in EL4 cells at the early stage of POX-induced apoptosis, which might involve Ca^{2+} efflux from the endoplasmic reticulum (ER) and Ca^{2+} influx from extracellular medium. Calcium signals and caspase-12 were important upstream messengers in POX-induced apoptosis in EL4 cells. The ER-associated pathway possibly operated in this apoptosis.

1. Introduction

Organophosphorus compounds (OPCs) are frequently utilized in agriculture, industry and medicine all over the world (Storm et al., 2000). Some OPCs are widespread environmental pollutants and potent toxic chemicals. To date, toxic effects and toxicological mechanisms of OPCs have been studied by many researchers both *in vitro* and *in vivo*. In recent years, more and more studies have indicated that induction of apoptosis is a new toxic effect of OPCs, and that apoptotic cell death may play an important role in OPC-induced impairing effects (Akbarsha and Sivasamy, 1998; Roy et al., 1998; Slotkin, 1999; Carlson et al., 2000; Bustos-Obregon et al., 2001; Masoud et al., 2003; Greenlee et al., 2004; Baille et al., 2005; Sharma et al., 2005; Wilczek, 2005; Oral et al., 2006; Yu et al., 2008). Therefore, it is necessary to elucidate the molecular mechanisms involved in OPC-induced apoptosis.

Apoptosis is an essential non-inflammatory mechanism for cell clearance, which occurs in both physiological and pathological processes. Apoptosis contains two major phases: the commitment phase (the early stage) and the execution phase (the late stage). In the commitment phase, apoptotic signals are transduced and no morphological changes are observed. In the execution phase, selective degradation of intracellular substrates occurs, and morphological changes such as cell collapse, formation of membrane blebs, chromatin condensation and fragmentation can be observed (Guo et al., 2005). The apoptotic process is tightly regulated by the balance of pro-apoptotic and anti-apoptotic signals (de Thonel and Eriksson, 2005). There are mainly three apoptotic signaling pathways that have been discovered: (1) the mitochondrial pathway (intrinsic pathway) (Desagher and Martinou, 2000; Wang, 2001); (2) the death receptor-associated pathway (extrinsic pathway) (Sidoti-de Fraisse et al., 1998; Sun et al., 1999); (3) the endoplasmic reticulum (ER)-associated pathway (Nakagawa et al., 2000; Szegezdi et al., 2003). Cellular Ca^{2+} has been strongly implicated in the induction and regulation of apoptosis. Although the work in this direction is far from being complete, numerous links that couple calcium to the extrinsic, intrinsic, and ER pathways of apoptosis have been discovered (Ermak and Davies, 2001; Berridge, 2002; Ferrari et al., 2002; Hajnóczky et al., 2003; Oakes et al., 2003; Prevarskaya et al., 2004; Guo et al., 2005; Sergeev, 2005; Hajnóczky et al., 2006).

Some researchers have investigated signaling pathways involved in OPC-induced apoptosis (Carlson et al., 2000; Masoud

Abbreviations: $[Ca^{2+}]i$, intracellular calcium concentration; cyt *c*, cytochrome *c*; ER, endoplasmic reticulum; IHC, immunohistochemistry; IP_3 R, inositol 1,4,5,-trisphosphate receptor; LSCM, laser scanning confocal microscopy; OD, optical density; OPCs, organophosphorus compounds; PBS, phosphate-buffered saline; POX, paraoxon; ROI, region of interest; Ry R, ryanodine receptor.

* Corresponding author. Tel.: +86 0931 8913240; fax: +86 0931 8912561.
E-mail address: wangzr@lzu.edu.cn (Z. Wang).

0887-2333/$ - see front matter © 2010 Elsevier Ltd. All rights reserved.
doi:10.1016/j.tiv.2010.01.005

et al., 2003; Saleh et al., 2003a,b; Caughlan et al., 2004; Wu et al., 2005; Chen et al., 2006; Nakadai et al., 2006; Li et al., 2007; Yu et al., 2008). However, to data, no one has investigated whether intracellular calcium signals operate at the early stage of OPC-induced apoptosis, and whether the ER-associated pathway is involved in this mechanism. Paraoxon (*O,O*-diethyl-*O*-4-nitrophenylphosphate, POX) is one of the most toxic organophosphorus pesticides. Its wide use in agriculture has made it a major cause of occupational and accidental intoxication (Stallones and Beseler, 2002; Vatanparast et al., 2006a). Many studies have shown that POX can influence intracellular Ca^{2+} signaling in several cultured cell lines (Sun et al., 2000; Hong et al., 2003; Vatanparast et al., 2006a,b, 2007; Qian et al., 2007). Saleh et al. (2003b) have established an experimental model in which POX at non-cholinergic doses (1–10 nM) can induce apoptosis in murine EL4 T-lymphocytic leukemia cells. Therefore, in the present study, we used the model established by Saleh et al. (2003b) to investigate whether intracellular Ca^{2+} participated in POX-induced apoptosis in EL4 cells as an upstream messenger, and whether the ER-associated pathway operated in this apoptosis, so that we could better elucidate the molecular mechanisms of POX-induced apoptosis.

We examined whether POX-induced apoptosis was linked to changes of intracellular Ca^{2+} homeostasis during the POX application (0–2 h) using real-time laser scanning confocal microscopy (LSCM). We also investigated apoptotic rates and morphological changes of EL4 cells after treatment with POX for 16 h. In addition, we evaluated expression of caspase-12, an initial caspase and a key element in the ER-associated pathway (Nakagawa et al., 2000; Szegezdi et al., 2003), by immunohistochemistry (IHC).

Major sources of intracellular Ca^{2+} are extracellular medium and the ER. Ca^{2+} efflux from ERs is mediated mainly through IP_3 receptor (IP_3 R)-associated Ca^{2+} channels and ryanodine receptor (Ry R)-associated Ca^{2+} channels (Mikoshiba, 1997; Ermak and Davies, 2001; Sergeev, 2005), and these channels distribute widely in all kinds of cells (Zhang et al., 2006). In the present research, EGTA was used to chelate Ca^{2+} in extracellular medium (Wang and Cai, 2003; Guo et al., 2005; Xiu et al., 2005). Heparin and procaine were used as specific antagonists to IP_3 R and Ry R, respectively, to inhibit Ca^{2+} efflux from the ER (Pu and Chang, 2001; Viets et al., 2001; Wang and Cai, 2003; Zhang et al., 2006).

2. Materials and methods

2.1. Chemicals and reagents

POX (*O,O*-diethyl-*O*-4-nitrophenylphosphate) was obtained from the Laboratories of Dr. Ehrenstorfer (Augsburg, Germany). Stock solution of POX (100 mM) was prepared in DMSO and stored at −80 °C. The working dilutions in phosphate-buffered saline (PBS) were prepared just before use. RPMI-1640 medium was purchased from Gibco Laboratories (Santa Clara, CA, USA). Fetal bovine serum was obtained from Si-Ji-Qing Biotechnology Co. (Hangzhou, Zhejiang, China). Fluo-3/AM and Hoechst 33258 were purchased from Molecular Probes Co. (Eugene, OR, USA). EGTA and heparin were purchased from Sigma Chemical Co. (St. Louis, MO, USA). Paraformaldehyde was obtained from Fluka Co., USA. Anti-caspase-12 rabbit polyclonal antibody was obtained from BioVision Co. (Mountain View, CA, USA). Anti-α-tubulin mouse monoclonal antibody was obtained from Beyotime Institute of Biotechnology (Haimen, Jiangsu, China). Normal goat serum working solution, biotinylated anti-rabbit goat IgG (secondary antibody) working solution, biotinylated anti-mouse goat IgG working solution and horseradish peroxidase-conjugated streptavidin working solution were purchased from Zhong-Shan Gold Bridge Biotechnology Co. (Beijing, China). The DAB kit was purchased from Boster Biotechnology Ltd. (Wuhan, Hubei, China). All other reagents are of analytical grade, made in China.

2.2. Cell culture

Murine EL4 T-lymphocytic leukemia cell line was purchased from the Cell Bank of Shanghai Institute of Cell Biology, Chinese Academy of Sciences (Shanghai, China). EL4 cells were grown in suspension in complete RPMI-1640 medium supplemented with 10% heat-inactivated fetal bovine serum, 100 units/ml penicillin, and 100 μg/ml streptomycin, and were kept at 37 °C in a humidified atmosphere of 5%CO_2/95% air in Yamato IP-41 CO_2 incubator (Japan). Cells were routinely passaged every other day. Prior to treatment, EL4 cells were harvested and seeded on plastic six-well culture plates at 5×10^5 cells/ml and allowed to grow for 24 h. After that, cells at logarithmic phase were ready for treatment.

2.3. Morphological features of apoptosis and the apoptotic rate assay

EL4 cells were divided into seven groups. Three groups were exposed to 1 nM, 5 nM, or 10 nM POX for 16 h. Three other groups were pre-treated with 1 mM EGTA (Xiu et al., 2005), 20 mg/ml heparin, or 1 mg/ml procaine (Zhang et al., 2006) for 2 h before exposure to 10 nM POX for 16 h. The control group was treated with the carrier solvent of POX (DMSO). Subsequently, cells were harvested by centrifugation at 400*g* for 8 min, washed with PBS, and fixed with 4% paraformaldehyde in PBS for 15 min. After fixation, cells were incubated in a 10 μg/ml Hoechst 33258 solution for 30 min at room temperature. The stained cells were spread on glass slides to make temporary mounting (Kim and Chung, 2008).

These slides were observed and photographed under a Zeiss LSM 510 META inverted laser scanning confocal microscope (Carl Zeiss, Germany). Differential-interference contrast microscopy and fluorescence microscopy were used to observe the morphology of the cell surface and nuclei. Hoechst 33258 stained cells were prepared for the evaluation of nuclear chromatin condensation and fragmentation. Random fields were selected to observe and count apoptotic cells. Nuclei displaying apoptotic characters were counted and compared numerically to morphologically normal nuclei in the same field. At least 200 cells were counted in each 200 × field. The percentage of apoptotic nuclei was calculated by the equation: (apoptotic nuclei/[apoptotic nuclei + normal nuclei]) × 100 (Kim and Chung, 2008). Every experiment was repeated for ten times. Data were expressed as mean ± SD, and analyzed using a Student's *t*-test. Significant differences compared to control groups were indicated by $^{*}(p \leqslant 0.05)$ or $^{**}(p \leqslant 0.01)$.

2.4. Real-time LSCM to monitor intracellular calcium signals

Fluo-3/AM was used to monitor changes of the intracellular calcium signaling in EL4 cells, during the application of POX or DMSO (control group) lasting for 2 h. Fluo-3/AM was dissolved in DMSO to make 1 mM stock solution, and stored at −80 °C.

Cells were divided into seven groups, and three of which were pre-treated with 1 mM EGTA, 20 mg/ml heparin, or 1 mg/ml procaine for 2 h. Subsequently, pre-treated and non-pre-treated cells were harvested by centrifugation at 400*g* for 8 min, washed twice with PBS, and incubated in 10 μM fluo-3/AM in RPMI-1640 medium (without phenolsulfonphthalein and fetal bovine serum) for 30 min at 37 °C. And then, cells were harvested by centrifugation at 400*g* for 8 min to remove the dye, washed twice with PBS, and re-suspended in RPMI-1640 medium mentioned above in 35 mm Petri dishes (Florea et al., 2007). Non-pre-treated groups were exposed to 1 nM, 5 nM, 10 nM POX, or 10 nM DMSO (control group). Pre-treated groups were exposed to 10 nM POX.

During the application of POX or DMSO (0–2 h), cells were monitored under a Zeiss LSM 510 META inverted laser scanning confocal microscope (Carl Zeiss, Germany) with an objective of 40×. The excitation wavelength was 488 nm and fluorescence readings for emission were at 525 nm for fluo-3. Fluorescence images were collected at room temperature (25 °C) every 5 min. Full screen images were taken to allow the analysis of the selected regions of interest (ROIs) offline (Florea et al., 2005).

Changes of intracellular calcium concentration ($[Ca^{2+}]i$) in selected individual cells during the application of POX or DMSO were illustrated by time courses, which were analyzed using the LSM 510 META software (Carl Zeiss). Two to four typical individual cells were shown in each plot. Changes of $[Ca^{2+}]i$ in cell groups were also illustrated by time courses. To display changes of $[Ca^{2+}]i$ in cell groups more clearly, results were shown as relative values of the fluorescence intensity from the control level (% of control). Each data point was an average value calculated from 15 to 54 samples. Data were expressed as mean ± SD. The maximal relative increment of calcium-sensitive dye fluorescence was calculated by the equation: $[(E/C - 1) \times 100]$, where C is the control level before treatment and E is the maximal exposure level during the application of POX or DMSO (Florea et al., 2005).

2.5. Assessment of caspase-12 expression by IHC

Cells were divided into six groups, and three of which were exposed to 1 nM, 5 nM or 10 nM POX for 0–16 h. Other groups were pre-treated with 1 mM EGTA, 20 mg/ml heparin, or 1 mg/ml procaine for 2 h, and all pre-treated groups were exposed to 10 nM POX for 0–16 h.

Subsequently, cells were harvested by centrifugation at 400*g* for 8 min, washed twice with cold PBS (stored at 4 °C), smeared on glass slides, air-dried and fixed with cold acetone (stored at 4 °C) for 10 min in humidified atmosphere. Cells on glass slides were washed twice with cold PBS and treated with 0.3%H_2O_2–methanol for 30 min at 4 °C in humidified atmosphere to inactivate the endogenous peroxidase. After two washes in cold PBS, cells on slides were blocked with normal goat serum working solution for 15 min at 4 °C in humidified atmosphere, and then incubated with anti-caspase-12 polyclonal antibody (dilution at 1:200) or anti-α-tubulin monoclonal antibody (dilution at 1:500) overnight at 4 °C in humidified atmosphere. A-tubulin was adopted as an internal control. After that, cells on slides were washed twice with cold PBS, incubated with biotinylated anti-rabbit goat IgG (secondary antibody) working solution for 12 min at room temperature in

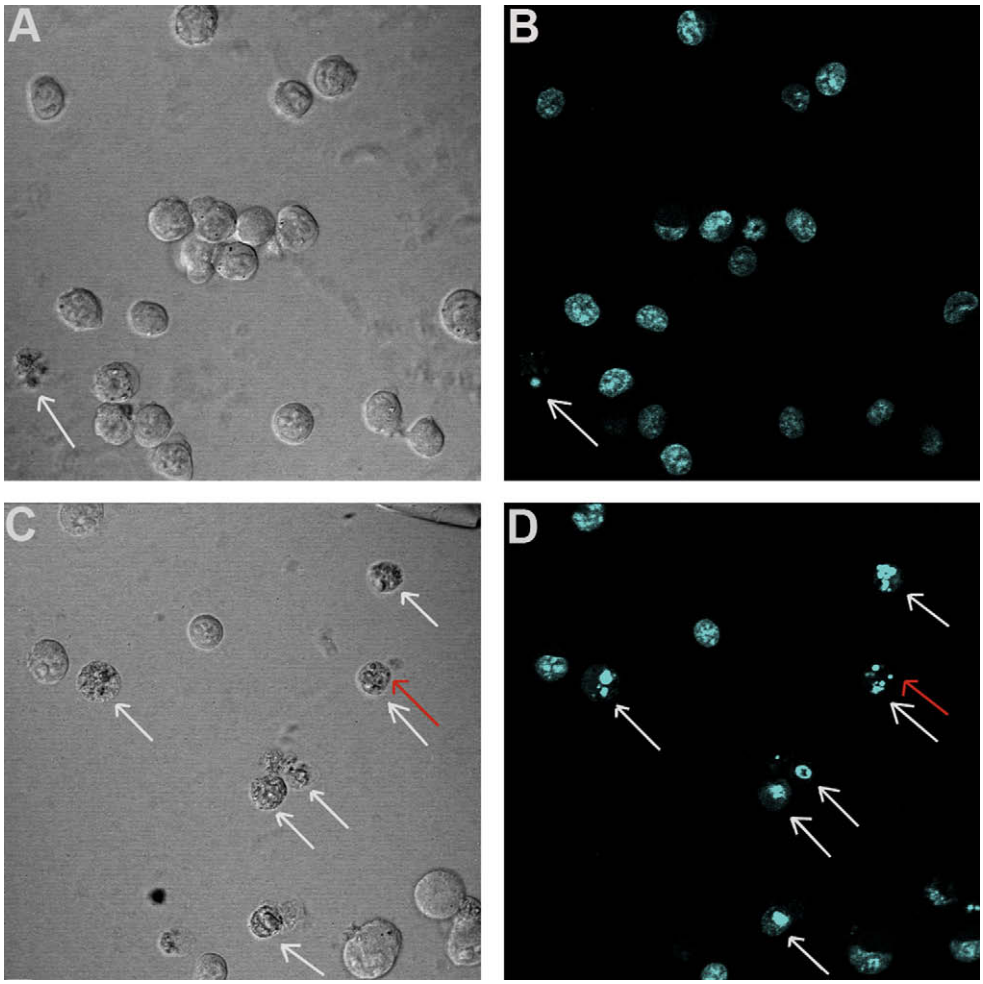

Fig. 1. *Morphological changes of EL4 cells after treatment with 10 nM POX for 16 h.* Cells were incubated in a 10 μg/ml Hoechst 33258 solution for 30 min at room temperature after paraformaldehyde fixation. (A) and (C) showed the surface morphology of cells observed by differential-interference contrast microscopy. (B) and (D) showed the nuclear morphology observed by fluorescence microscopy. (A) and (B) Control cells with normal morphology. (C) Cells treated with 10 nM POX for 16 h were shrunken accompanied with blebbing of cell membrane. (D) Cells treated with 10 nM POX for 16 h showed irregular chromatin condensation or fragmentation. White arrows indicate late stage apoptotic cells, and red arrows indicate buds which would form apoptotic bodies. Original magnification: ×200.

humidified atmosphere, washed twice with cold PBS again, and then incubated with horseradish peroxidase-conjugated streptavidin working solution for 10 min at room temperature in humidified atmosphere. Finally, the DAB kit was used to develop the visual signal. Cells on slides were then dehydrated with ethanol, cleared in xylene and mounted in resin.

These slides were observed and photographed under an Olympus light microscope (Olympus, Japan) with an objective of 40×. To assess the intensity of immunoreactivity, levels of staining were quantified using Image Pro-Plus 6.0 software (Media Cybernetics Inc., USA). Values of optical density (OD) in individual cells represented quantities of objective proteins, and were calculated by the equation: [(∑IOD)/(∑Area)], in which IOD is the integral optical density in a region of interest (ROI), and Area is the area of a ROI. In this study, a ROI represents an individual cell. ∑Area is the total area of all cells in the photograph, and ∑IOD is the sum of integral optical density of all cells in the photograph (Xavier et al., 2005). To display changes of protein expression more clearly, results were shown as relative values of the protein expression from the control level (% of control). Data were expressed as mean ± SD, and analyzed using a Student's *t*-test. Significant differences compared to control were indicated by $^{*}(p \leqslant 0.05)$ or $^{**}(p \leqslant 0.01)$. Every experiment was repeated for nine times.

3. Results

3.1. The morphology assay and the apoptotic rate assay of POX-induced apoptosis in EL4 cells

The morphology assay showed that POX induced typical apoptotic morphological changes in EL4 cells (Fig. 1). Cells in the control group showed normal morphological features: their nuclei were stained heterogeneously with Hoechst 33258 and the plasma membrane was smooth (Fig. 1A and B). In the group exposed to 10 nM POX for 16 h, many cells exhibited irregular chromatin condensation or nuclear fragmentation, and the cell surface became coarse because of shrinking, budding and/or blebbing of the plasma membrane (Fig. 1C and D).

The apoptotic rate assay showed that apoptotic rates of EL4 cells after treatment with 1–10 nM POX for 16 h increased significantly compared to the control group. There was a concentration-dependent increase of the apoptotic rate of EL4 cells from low to high POX concentrations (Fig. 2A). Pre-treatment with EGTA, heparin, or procaine significantly attenuated POX-induced apoptosis in EL4 cells, suggesting that the inhibition of $[Ca^{2+}]i$ elevation could attenuate this process (Fig. 2B) and $[Ca^{2+}]i$ elevation was intimately linked to the onset of apoptosis. However, apoptotic rates of pre-treated groups shown in Fig. 2B were significantly higher than the control group (10 nM DMSO, 16 h).

3.2. POX-induced changes of $[Ca^{2+}]i$ in EL4 cells detected by real-time LSCM

Changes of $[Ca^{2+}]i$ in EL4 cells during the application of POX (0–2 h) were detected by real-time LSCM. Changes of $[Ca^{2+}]i$ in individual cells and cell groups were shown in Figs. 3 and 4, respectively.

In individual cells, POX rapidly enhanced intracellular calcium signaling in a dose-dependent manner (Fig. 3A–D). Amplitude, duration, localization, and frequency of Ca^{2+} oscillations are elements which form a complex code of calcium signaling (Sergeev, 2005). Our results showed that, compared to the control group, POX at lower concentration (1 nM) mainly increased the amplitude of Ca^{2+} oscillations in EL4 cells (Fig. 3A and B), and POX at higher concentrations (5 nM and 10 nM) increased both the amplitude and the duration of Ca^{2+} oscillations (Fig. 3A, C and D). POX at 5 nM concentration induced a sustained increase of $[Ca^{2+}]i$ which rapidly reached a plateau. The plateau maintained for about 1 h or longer, and then $[Ca^{2+}]i$ decreased gradually and slowly until the end of POX application. POX at 10 nM concentration induced a sustained increase of $[Ca^{2+}]i$ during its application. Fig. 5 showed that fluo-3 fluorescence intensity in EL4 cells gradually increased during the 10 nM POX application. Therefore, compared to 5 nM POX, 10 nM POX induced a higher increase of $[Ca^{2+}]i$ in EL4 cells. In cell groups, POX-induced changes of $[Ca^{2+}]i$ were similar to those in individual cells (Fig. 4A–D). The maximal relative increment of $[Ca^{2+}]i$ from the control level (0 min) increased with increasing POX concentration (Fig. 4H1), that also supports the conclusion that POX enhanced intracellular calcium signaling in a dose-dependent manner.

In individual cells, pre-treatment with EGTA, heparin, or procaine significantly attenuated the POX-induced enhancement of

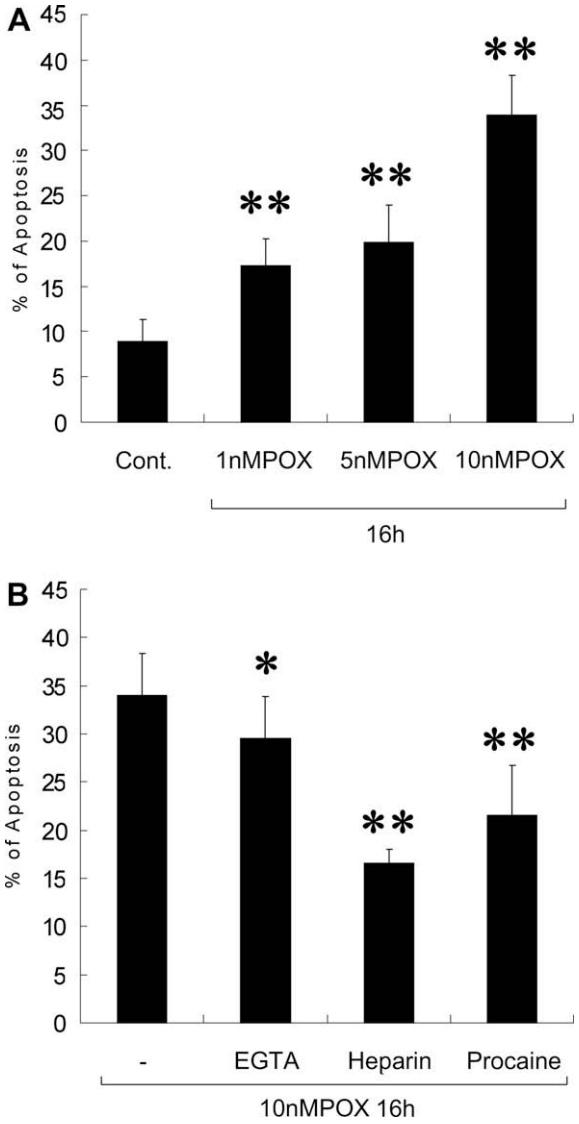

Fig. 2. *Apoptotic rates of EL4 cells after treatment with POX for 16 h.* (A) EL4 cells treated with 1 nM, 5 nM, 10 nM POX or 10 nM DMSO for 16 h. (B) EL4 cells treated with 10 nM POX for 16 h after pre-treatment with 1 mM EGTA, 20 mg/ml heparin or 1 mg/ml procaine for 2 h, or without any pre-treatment. The group treated with 10 nM DMSO for 16 h acted as the control group in (A), and the group treated with 10 nM POX for 16 h acted as the control group in (B). $n = 10$. Statistically significant differences compared to the control groups were indicated by asterisks: $^{*}p \leqslant 0.05$ and $^{**}p \leqslant 0.01$.

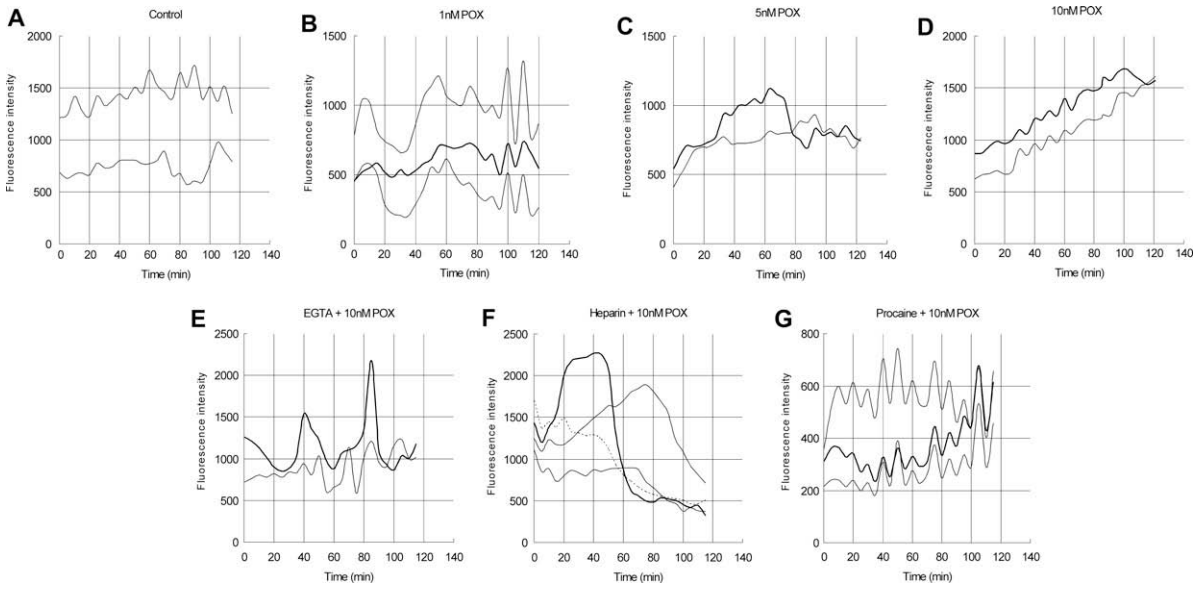

Fig. 3. *Changes of [Ca^{2+}]i in selected individual cells induced by POX within 2 h.* Changes of [Ca^{2+}]i were detected by real-time LSCM. Cells were incubated in a 10 μM fluo-3/AM solution at 37 °C for 30 min before exposure to POX or DMSO. (A) Control group: EL4 cells exposed to 10 nM DMSO. (B)–(D) EL4 cells exposed to 1 nM (B), 5 nM (C) or 10 nM (D) POX; (E)–(G) EL4 cells pre-treated with 1 mM EGTA (E), 20 mg/ml heparin (F), or 1 mg/ml procaine (G) for 2 h before exposure to 10 nM POX. The time courses were analyzed using the META software (Zeiss). They illustrated changes of [Ca^{2+}]i in selected regions of interest (ROIs), during the application of POX or DMSO. In the present study, one ROI represents an individual cell. Two to four individual cells were shown in each plot. At the beginning of POX (or DMSO) application, fluorescence intensities in individual cells were different, because cells were in different physiological states.

intracellular calcium signaling (Fig. 3D–G). In non-pre-treated cells, 10 nM POX induced a sustained increase of [Ca^{2+}]i until the end of its application (Fig. 3D), which was impaired by pre-treatment with EGTA (Fig. 3E), heparin (Fig. 3F), or procaine (Fig. 3G). As shown in Fig. 4D–G, POX-induced changes of [Ca^{2+}]i in pre-treated cell groups were similar to those in individual cells. During the 10 nM POX application, both the amplitude and the duration of intracellular calcium signaling decreased in pre-treated cells, compared to non-pre-treated cells. Data in Fig. 4H2 also support the conclusion mentioned above. The maximal relative increment of [Ca^{2+}]i from the control level (0 min) decreased in pre-treated groups, compared to the non-pre-treated group.

3.3. POX-induced changes of caspase-12 expression in EL4 cells detected by IHC

Immunohistochemical experiments were performed to investigate changes of caspase-12 expression in EL4 cells during the POX application (0–16 h), and data were semiquantitatively evaluated by densitometry using IPP 6.0 software.

In 1 nM POX-treated cells, caspase-12 expression after treatment for 2 h or 4 h was similar to the control (0 h), but caspase-12 expression after treatment for 8 h or 16 h was significantly higher than the control (Fig. 6A). During the application of 5 nM POX for 0–8 h, caspase-12 expression increased significantly and continuously, and reached the peak after 8 h treatment. However, caspase-12 expression after treatment with 5 nM POX for 16 h was similar to the control (Fig. 6A). The trend of changes of caspase-12 expression during the 10 nM POX application was similar to that during the 5 nM POX application, but increments of caspase-12 expression in 10 nM POX-treated cells were much higher than those in 5 nM POX-treated cells (Fig. 6A). In conclusion, we found that there was a tendency towards a concentration-dependent increase of caspase-12 expression in EL4 cells from low to high POX concentrations, and POX at higher concentrations increased the caspase-12 expression more quickly.

We then examined 10 nM POX-induced changes of caspase-12 expression in cells pre-treated with EGTA, heparin, or procaine. During the 10 nM POX application, caspase-12 expression in EGTA-pre-treated cells increased slowly and persistently, but the maximal increment of caspase-12 expression was much lower than that in non-pre-treated cells (Fig. 6B). No significant changes of caspase-12 expression were observed in heparin-pre-treated cells during the 10 nM POX application (Fig. 6B). The trend of changes of caspase-12 expression in procaine-pre-treated cells was similar to that in non-pre-treated cells during the 10 nM POX application, but increments of caspase-12 expression were much smaller than those in non-pre-treated cells (Fig. 6B). In conclusion, pre-treatment with EGTA, heparin, or procaine significantly attenuated the POX-induced increase of caspase-12 expression in EL4 cells.

4. Discussion

Researchers have been focusing on toxic effects and toxicological mechanisms of OPCs, because of their wide uses and environmental damages. In recent years, researchers have demonstrated that OPC induce apoptosis both *in vitro* and *in vivo*, which may play an important role in OPC-induced impairment, and some researchers have investigated signaling pathways involved in this apoptosis. Ca^{2+} has been proved to be an important messenger in apoptosis, and the ER-associated pathway has been suggested to be a major apoptotic pathway. [Ca^{2+}]i elevation has been observed at the late stage of OPC-induced apoptosis (Chen et al., 2006; Yu et al., 2008), but not at the early stage, and no one has studied whether the ER-associated pathway is involved in this apoptosis.

In this study, we found that 1–10 nM POX induced apoptosis in EL4 cells in a dose-dependent manner (Fig. 2A), and enhanced the intracellular calcium signaling in a similar manner at the early stage of apoptosis (Figs. 3A–D, 4A–D and H1). Inhibiting the POX-induced [Ca^{2+}]i elevation could significantly attenuate this apoptosis (Fig. 2B). These results suggested that intracellular Ca^{2+} was a potent upstream pro-apoptotic messenger acting at the early stage of POX-induced apoptosis in EL4 cells.

In our experiments, EGTA was used to chelate Ca^{2+} in extracellular medium. Heparin and procaine were used as specific antago-

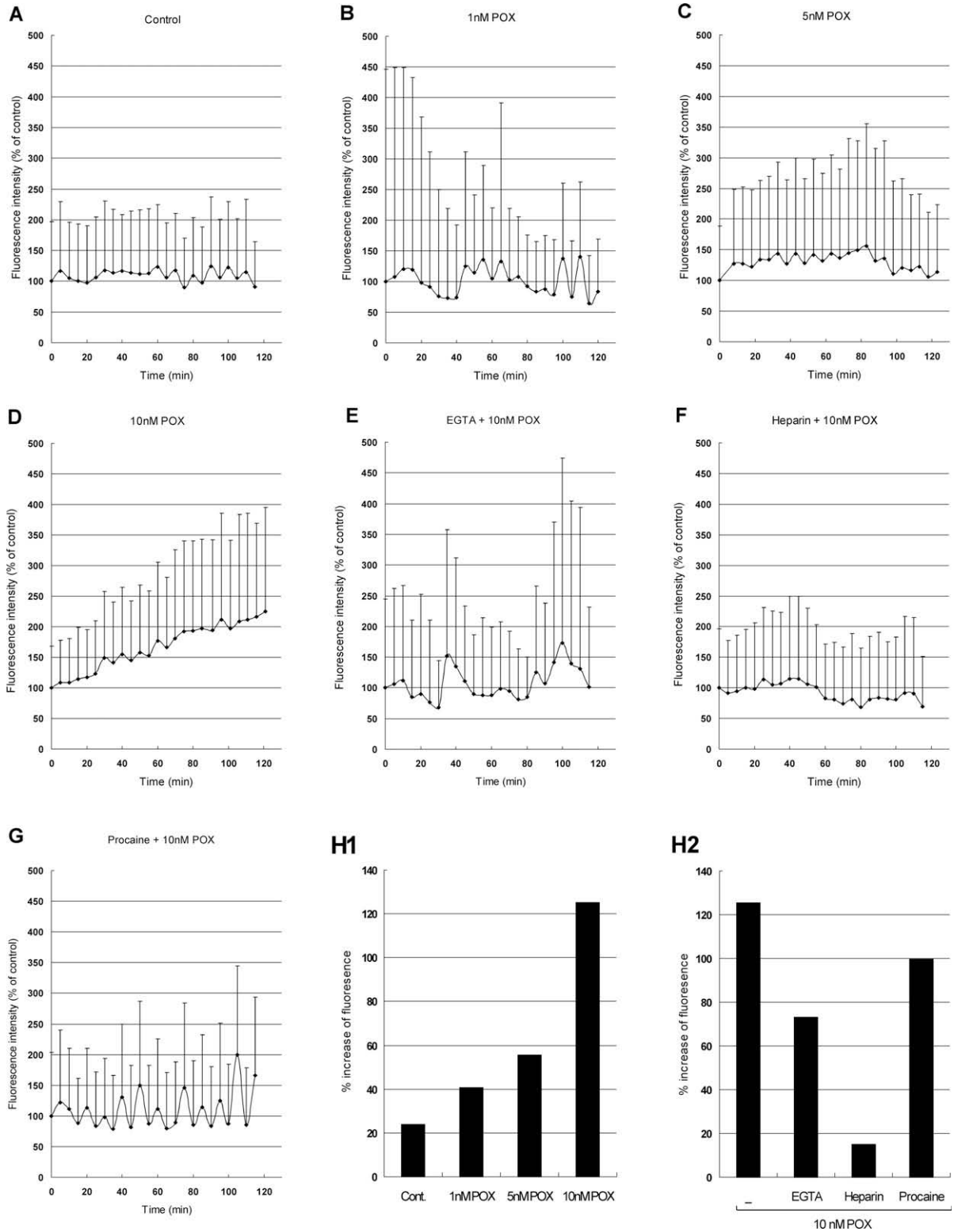

Fig. 4. *Changes of [Ca²⁺]i in cell groups induced by POX within 2 h.* Changes of [Ca^{2+}]i were detected by real-time LSCM (A–G). Cells were incubated in a 10 μM fluo-3/AM solution at 37 °C for 30 min before exposure to POX or DMSO. (A) Control group: EL4 cells exposed to 10 nM DMSO. (B)–(D) EL4 cells exposed to 1 nM (B), 5 nM (C) or 10 nM (D) POX. (E)–(G) EL4 cells pre-treated with 1 mM EGTA (E), 20 mg/ml heparin (F) or 1 mg/ml procaine (G) for 2 h before exposure to 10 nM POX. Data were expressed as mean ± SD. Each data point was an average value calculated from 15 to 54 samples. The maximal increments of fluo-3 fluorescence in EL4 cells during the application of POX or DMSO, compared to the fluorescence intensity before exposure to POX or DMSO, were shown in H1 and H2. (H1) EL4 cells exposed to 1 nM, 5 nM, 10 nM POX or 10 nM DMSO (control group); (H2) EL4 cells exposed to 10 nM POX after pre-treatment with 1 mM EGTA, 20 mg/ml heparin or 1 mg/ml procaine for 2 h, or without any pre-treatment Data in H1 and H2 were calculated from data shown in A–G, so there are no error bars in H1 and H2, and no statistical tests were carried out.

nists to IP_3 R and Ry R, respectively, to inhibit Ca^{2+} efflux from the ER. All of the three pre-treatments attenuated the POX-induced [Ca^{2+}]i elevation at the early stage of this apoptosis (Figs. 3D–G, 4D–G and H2), and partially inhibited apoptosis (Fig. 2B). These re-

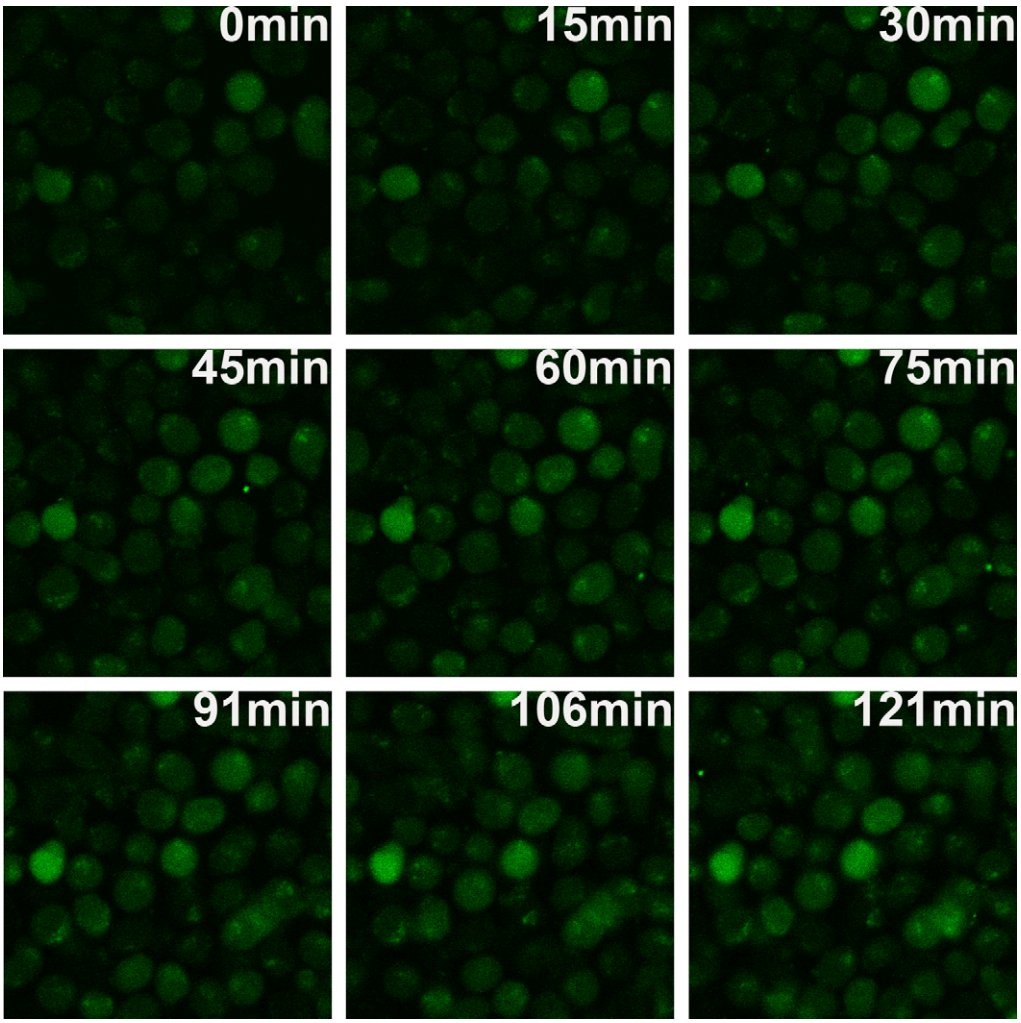

Fig. 5. *Changes of the intensity of fluo-3 fluorescence during the 10 nM POX application*. Cells were incubated in a 10 μM fluo-3/AM solution for 30 min at 37 °C before exposure to POX. Images were captured under an inverted laser scanning confocal microscope. EL4 cells were exposed to 10 nM POX. During the whole period of 10 nM POX application, the intensity of intracellular fluo-3 fluorescence increased gradually and continuously. Original magnification: ×400.

sults suggested that Ca^{2+} influx from extracellular medium and Ca^{2+} efflux from the ER were both involved in the POX-induced enhancement of intracellular calcium signaling, and the POX-induced Ca^{2+} efflux from ERs was through both IP_3 R-associated Ca^{2+} channels and Ry R-associated Ca^{2+} channels.

We found that 1–10 nM POX increased caspase-12 expression in EL4 cells in a dose-dependent manner (Fig. 6A), 5 nM and 10 nM POX significantly increased the caspase-12 expression within 2 h (Fig. 6A). Additionally, we found that inhibiting the POX-induced [Ca^{2+}]i elevation suppressed the POX-induced apoptosis and increase of caspase-12 expression to different degrees (Figs. 2B and 6B) These results suggested that caspase-12 was an upstream pro-apoptotic messenger acting at the early stage of POX-induced apoptosis in EL4 cells, and was a target of intracellular Ca^{2+}. Because caspase-12 is an initial caspase in the ER-associated pathway (Nakagawa et al., 2000; Szegezdi et al., 2003), our results suggested that this pathway possibly operated in the apoptosis.

On all accounts, this study enriches our knowledge of molecular mechanisms involved in POX-induced apoptosis in EL4 cells, and following conclusions were obtained for the first time. At the early stage of POX-induced apoptosis in EL4 cells, calcium signaling was significantly enhanced as a pivotal upstream pro-apoptotic messenger. The POX-induced [Ca^{2+}]i elevation came from two sources: extracellular medium and ERs, and Ca^{2+} efflux from the ER was mainly through IP_3 R-associated Ca^{2+} channels and Ry R-associated Ca^{2+} channels. As a target of intracellular Ca^{2+}, the expression of caspase-12 rapidly increased at the early stage of this apoptosis, and the ER-associated pathway possibly operated in this apoptosis.

In heparin-pre-treated cells, POX-induced apoptosis was only inhibited partially, whereas POX-induced increase of caspase-12 expression during the POX application (0–16 h) was completely suppressed (Figs. 2B and 6B). These data indicated that besides ER-associated pathway, other signaling pathways might also participate in POX-induced apoptosis in EL4 cells. This is consistent with the report that POX induced apoptosis in EL4 cells through activation of mitochondrial pathways (Saleh et al., 2003b).

According to Saleh et al. (2003b), POX at non-cholinergic doses (1–10 nM) caused apoptosis in EL4 cells via activation of mitochondrial pathways, in which cytochrome *c* (cyt *c*) release to cytoplasm is an important pro-apoptotic event. However, how cyt *c* was released from mitochondria needs to be investigated. Some studies have indicated that ERs and mitochondria form a highly dynamic interconnected network in which they cooperate to generate Ca^{2+} signals. [Ca^{2+}]i elevation-induced Ca^{2+} accumulation in mitochondria may disturb the balance of physiological activities in mitochondria and trigger the cyt *c* release (Ermak and Davies, 2001; Berridge, 2002; Hajnóczky et al., 2006). Results of Saleh et al. (2003b) have shown that cyt *c* release began after treatment with

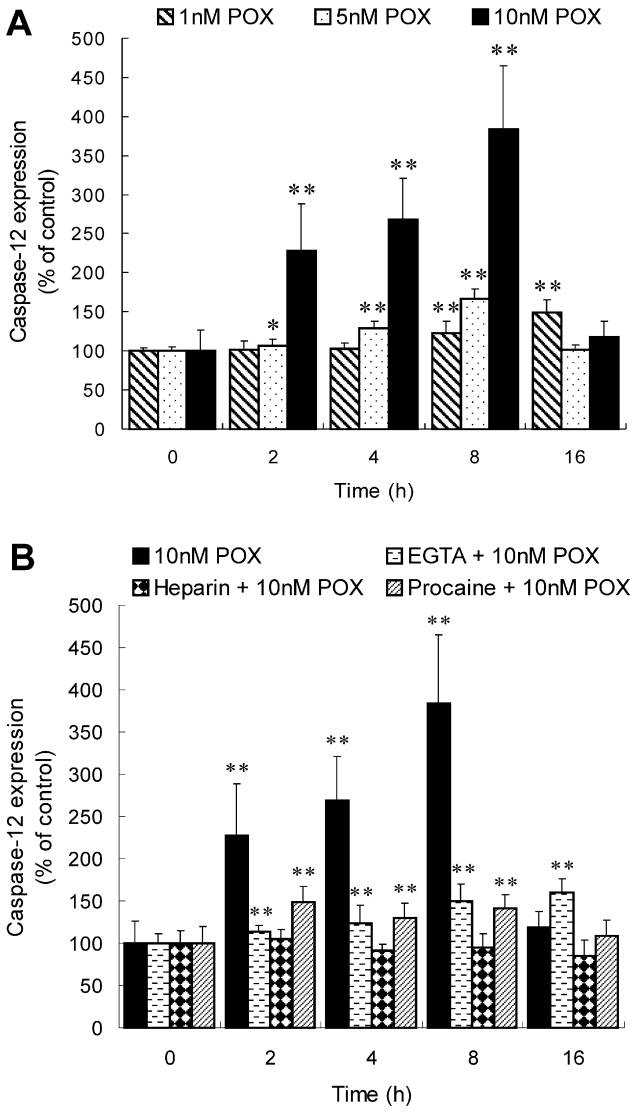

Fig. 6. *Changes of caspase-12 expression in EL4 cells during the POX application (0–16 h), detected by IHC.* (A) EL4 cells treated with 1nM, 5nM or 10 nM POX; (B) EL4 cells treated with 10 nM POX after pre-treatment with 1 mM EGTA, 20 mg/ml heparin or 1 mg/ml procaine for 2 h, or without any pre-treatment. $n = 9$. Statistically significant differences compared to control (0 h) were indicated by asterisks: $^{*}p \leqslant 0.05$ and $^{**}p \leqslant 0.01$.

10 nM POX for 4 h. Our results showed that $[Ca^{2+}]i$ elevation occurred within 2 h after 10 nM POX application. Therefore, the POX-induced $[Ca^{2+}]i$ elevation occurred earlier than cyt *c* release. In future studies, it will be important to clarify whether the POX-induced $[Ca^{2+}]i$ elevation can trigger cyt *c* efflux from mitochondria. In other words, we should investigate whether the ER/mitochondria cross-talk participate in POX-induced apoptosis in EL4 cells. Additionally, in future studies, it is necessary to elucidate how the ER-associated pathway operates in this apoptosis.

5. Conflict of interest

The authors declare that there are no conflicts of interest.

Acknowledgements

We thank Dr. Shengxiang Zhang for his valuable suggestions and feedback on this manuscript. This work was supported by the grant (No. 30670230) from the National Natural Science Foundation of China to ZW.

References

Akbarsha, M.A., Sivasamy, P., 1998. Male reproductive toxicity of phosphamidon: histopathological changes in epididymis. Indian Journal of Experimental Biology 36, 34–38.

Baille, V., Clarke, P.G.H., Brochier, G., Dorandeu, F., Verna, J.M., Four, E., Lallement, G., Carpentier, P., 2005. Soman-induced convulsions: the neuropathology revisited. Toxicology 215, 1–24.

Berridge, M.J., 2002. The endoplasmic reticulum: a multifunctional signaling organelle. Cell Calcium 32, 235–249.

Bustos-Obregon, E., Diaz, O., Sobarzo, C., 2001. Parathion induces mouse germ cells apoptosis. Italian Journal of Anatomy and Embryology 106 (2 Suppl. 2), 199–204.

Carlson, K., Jortner, B.S., Ehrich, M., 2000. Organophosphorus compound-induced apoptosis in SH-SY5Y human neuroblastoma cells. Toxicology and Applied Pharmacology 168, 102–113.

Caughlan, A., Newhouse, K., Namgung, U., Xia, Z., 2004. Chlorpyrifos induces apoptosis in rat cortical neurons that is regulated by a balance between p38 and ERK/JNK MAP kinases. Toxicological Sciences 78, 125–134.

Chen, X., Shao, J., Xiang, L., Liu, X., 2006. Involvement of apoptosis in malathion-induced cytotoxicity in a grass carp (*Ctenopharyngodon idellus*) cell line. Comparative Biochemistry and Physiology C – Toxicology and Pharmacology 142, 36–45.

de Thonel, A., Eriksson, J.E., 2005. Regulation of death receptors – relevance in cancer therapies. Toxicology and Applied Pharmacology 207, S123–S132.

Desagher, S., Martinou, J.C., 2000. Mitochondria as the central control point of apoptosis. Trends in Cell Biology 10, 369–377.

Ermak, G., Davies, K.J.A., 2001. Calcium and oxidative stress: from cell signaling to cell death. Molecular Immunology 38, 713–721.

Ferrari, D., Pinton, P., Szabadkai, G., Chami, M., Campanella, M., Pozzan, T., Rizzuto1, R., 2002. Endoplasmic reticulum, Bcl-2 and Ca^{2+} handling in apoptosis. Cell Calcium 32, 413–420.

Florea, A.M., Splettstoesser, F., Dopp, E., Rettenmeier, A.W., Büsselberg, D., 2005. Modulation of intracellular calcium homeostasis by trimethyltin chloride in human tumour cells: neuroblastoma SY5Y and cervix adenocarcinoma HeLa S3. Toxicology 216, 1–8.

Florea, A.M., Splettstoesser, F., Büsselberg, D., 2007. Arsenic trioxide (As_2O_3) induced calcium signals and cytotoxicity in two human cell lines: SY-5Y neuroblastoma and 293 embryonic kidney (HEK). Toxicology and Applied Pharmacology 220, 292–301.

Greenlee, A.R., Ellis, T.M., Berg, R.L., 2004. Low-dose agrochemicals and lawn-carepesticides induce developmental toxicity in murine preimplantation embryos. Environmental Health Perspectives 112, 703–709.

Guo, J., Pu, Y., Zhang, D., 2005. Calcium signaling in apoptosis. Acta Biophysica Sinica 21, 1–18.

Hajnóczky, G., Davies, E., Madesh, M., 2003. Calcium signaling and apoptosis. Biochemical and Biophysical Research Communications 304, 445–454.

Hajnóczky, G., Csordás, G., Das, S., Garcia-Perez, C., Saotome, M., Roy, S.S., Yi, M., 2006. Mitochondrial calcium signalling and cell death: Approaches for assessing the role of mitochondrial Ca^{2+} uptake in apoptosis. Cell Calcium 40, 553–560.

Hong, M.S., Hong, S.J., Barhoumi, R., Burghardt, R.C., Donnelly, K.C., Wild, J.R., Venkatraj, V., Tiffany-Castiglioni, E., 2003. Neurotoxicity induced in differentiated SK-N-SH-SY5Y human neuroblastoma cells by organophosphorus compounds. Toxicology and Applied Pharmacology 186, 110–118.

Kim, B.M., Chung, H.W., 2008. Desferrioxamine (DFX) induces apoptosis through the p38-caspase8-Bid-Bax pathway in PHA-stimulated human lymphocytes. Toxicology and Applied Pharmacology 228, 24–31.

Li, Q., Kobayashi, M., Kawada, T., 2007. Organophosphorus pesticides induce apoptosis in human NK cells. Toxicology 239, 89–95.

Masoud, L., Vijayasarathy, C., Fernandez-Cabezudo, M., Petroianu, G., Saleh, A.M., 2003. Effect of malathion on apoptosis of murine L929 fibroblasts: a possible mechanism for toxicity in low dose exposure. Toxicology 185, 89–102.

Mikoshiba, K., 1997. The $InsP_3$ receptor and intracellular Ca^{2+} signaling. Current Opinion in Neurobiology 7, 339–345.

Nakadai, A., Li, Q., Kawada, T., 2006. Chlorpyrifos induces apoptosis in human monocyte cell line U937. Toxicology 224, 202–209.

Nakagawa, T., Zhu, H., Morishima, N., Li, E., Xu, J., Yankner, B.A., Yuan, J., 2000. Caspase-12 mediates endoplasmic-reticulum-specific apoptosis and cytotoxicity by amyloid-beta. Nature 403, 98–103.

Oakes, S.A., Opferman, J.T., Pozzan, T., Korsmeyer, Scorrano L., 2003. Regulation of endoplasmic reticulum Ca^{2+} dynamics by proapoptotic BCL-2 family members. Biochemical Pharmacology 66, 1335–1340.

Oral, B., Guney, M., Demirin, H., Ozguner, M., Giray, S.G., Take, G., Mungan, T., Altuntas, I., 2006. Endometrial damage and apoptosis in rats induced by dichlorvos and ameliorating effect of antioxidant Vitamins E and C. Reproductive Toxicology 22, 783–790.

Prevarskaya, N., Skryma, R., Shuba, Y., 2004. Ca^{2+} homeostasis in apoptotic resistance of prostate cancer cells. Biochemical and Biophysical Research Communications 322, 1326–1335.

Pu, Y., Chang, D.C., 2001. Cytosolic Ca^{2+}signal is involved in regulating UV-induced apoptosis in HeLa cells. Biochemical and Biophysical Research Communications 282, 84–89.

Qian, Y., Venkatraj, J., Barhoumi, R., Pal, R., Datta, A., Wild, J.R., Tiffany-Castiglioni, E., 2007. Comparative non-cholinergic neurotoxic effects of paraoxon and diisopropyl fluorophosphate (DFP) on human neuroblastoma and astrocytoma cell lines. Toxicology and Applied Pharmacology 219, 162–171.

Roy, T.S., Andrews, J.E., Seidler, F.J., Slotkin, T.A., 1998. Chlorpyrifos elicits mitotic abnormalities and apoptosis in neuroepithelium of cultured rat embryos. Teratology 58, 62–68.

Saleh, A.M., Vijayasarathy, C., Fernandez-Cabezudo, M., Taleb, M., Petroianu, G., 2003a. Influence of paraoxon (POX) and parathion (PAT) on apoptosis: a possible mechanism for toxicity in low dose exposure. Journal of Applied Toxicology 23, 23–29.

Saleh, A.M., Vijayasarathy, C., Masoud, L., Kumar, L., Shahin, A., Kambal, A., 2003b. Paraoxon induces apoptosis in EL4 cells via activation of mitochondrial pathways. Toxicology and Applied Pharmacology 190, 47–57.

Sergeev, I.N., 2005. Calcium signaling in cancer and vitamin D. Journal of Steroid Biochemistry and Molecular Biology 97, 145–151.

Sharma, Y., Bashir, S., Irshad, M., Nag, T.C., Dogra, T.D., 2005. Dimethoate-induced effects on antioxidant status of liver and brain of rats following subchronic exposure. Toxicology 215, 173–181.

Sidoti-de Fraisse, C., Rincheval, V., Risler, Y., Mignotte, B., Vayssiere, J.L., 1998. TNF-alpha activates at least two apoptotic signaling cascades. Oncogene 17, 1639–1651.

Slotkin, T.A., 1999. Developmental cholinotoxicants: nicotine and chlorpyrifos. Environmental Health Perspectives 107 (Suppl. 1), 71–80.

Stallones, L., Beseler, C., 2002. Pesticide illness, farm practices, and neurological symptoms among farm residents in Colorado. Environmental Research 90, 89–97.

Storm, J.E., Karl, K.R., Doull, J., 2000. Occupational exposure limits for 30 organophosphate pesticides based on inhibition of red cell acetylcholinesterase. Toxicology 150, 1–29.

Sun, X.M., MacFarlane, M., Zhuang, J., Wolf, B.B., Green, D.R., Cohen, G.M., 1999. Distinct caspase cascades are initiated in receptor-mediated and chemical-induced apoptosis. Journal of Biological Chemistry 274, 5053–5060.

Sun, X., Liu, X.B., Martinez, J.R., Zhang, G.H., 2000. Effects of low concentrations of paraoxon on Ca^{2+} mobilization in a human parotid salivary cell-line HSY. Archives of Oral Biology 45, 621–638.

Szegezdi, E., Fitzgerald, U., Samali, A., 2003. Caspase-12 and ER-stress-mediated apoptosis: the story so far. Annals of the New York Academy of Sciences 1010, 186–194.

Vatanparast, J., Janahmadi, M., Asgari, A.R., 2006a. The functional consequences of paraoxon exposure in central neurones of land snail, *Caucasotachea atrolabiata*, are partly mediated through modulation of Ca^{2+} and Ca^{2+}-activated K^+-channels. Comparative Biochemistry and Physiology C – Toxicology and Pharmacology 143, 464–472.

Vatanparast, J., Janahmadi, M., Asgari, A.R., Sepehri, H., Haeri-Rohani, A., 2006b. Paraoxon suppresses Ca^{2+} spike and after hyperpolarization in snail neurons: Relevance to the hyperexcitability induction. Brain Research 1083, 110–117.

Vatanparast, J., Janahmadi, M., Asgari, A.R., 2007. Involvement of protein kinase C and IP3-mediated Ca^{2+} release in activity modulation by paraoxon in snail neurons. European Journal of Pharmacology 571, 81–87.

Viets, L.N., Campbell, K.D., White, K.L., 2001. Pathways involved in RGD-mediated calcium transients in mature bovine oocytes. Cloning and Stem Cells 3, 105–113.

Wang, X., 2001. The expanding role of mitochondria in apoptosis. Genes and Development 15, 2922–2933.

Wang, H., Cai, H.R., 2003. Modulation of extracellular calcium on miniature inhibitory postsynaptic currents of Xenopus' optic tectal neurons. Acta Physiology Sinica 55, 599–606.

Wilczek, G., 2005. Apoptosis and biochemical biomarkers of stress in spiders from industrially polluted areas exposed to high temperature and dimethoate. Comparative Biochemistry and Physiology C – Toxicology and Pharmacology 141, 194–206.

Wu, X., Tian, F., Okagaki, P., Marini, A.M., 2005. Inhibition of *N*-methyl-D-aspartate receptors increases paraoxon-induced apoptosis in cultured neurons. Toxicology and Applied Pharmacology 208, 57–67.

Xavier, L.L., Viola, G.G., Ferraz, A.C., Da Cunha, C., Deonizio, J.M.D., Netto, C.A., Achaval, M., 2005. A simple and fast densitometric method for the analysis of tyrosine hydroxylase immunoreactivity in the substantia nigra pars compacta and in the ventral tegmental area. Brain Research Protocols 16, 58–64.

Xiu, M., Peng, J., Hong, H., 2005. Reactions of mitochondria and changes of Ca^{2+} in the baculovirus-induced apoptosis in entomic cells. Chinese Science Bulletin 50, 1213–1219.

Yu, F., Wang, Z., Ju, B., Wang, Y., Wang, J., Bai, D., 2008. Apoptotic effect of organophosphorus insecticide chlorpyrifos on mouse retina in vivo via oxidative stress and protection of combination of vitamins C and E. Experimental and Toxicologic Pathology 59, 415–442.

Zhang, M., Wang, J.J., Chen, Y.J., 2006. Effects of mechanical pressure on intracellular calcium release channel and cytoskeletal structure in rabbit mandibular condylar chondrocytes. Life Science 78, 2480–2487.